SUPPORTING INFORMATION

Polymeric Nano-Thermometer Exploiting Reverse Intersystem Crossing: A Potential Solution to Common Interferences

Anwesha Banerjee, [†] Akash Kumar Parida, [†] Anirban Panda,[‡] Dibyendu Mallick,[§] Ujjal Bhattacharjee [*,†]

[†]Department of Chemistry, Indian Institute of Engineering Science and Technology (IIEST) Shibpur, Howrah, West Bengal 711103, India.

[§]Presidency University, Kolkata, West Bengal, 700073, India.

[‡]Jagannath Kishore College, Purulia, West Bengal 723101, India.

[*]Email: ujjalb.chem@faculty.iiests.ac.in

Figure S1.

In this figure, normalized excited state lifetime decay of eosin y was taken in TCSPC module in HORIBA Fluorolog-3 in ethanol with an excitation wavelength of 505 nm and emission wavelength was taken at 540 nm with a lifetime of 1.2 ns.

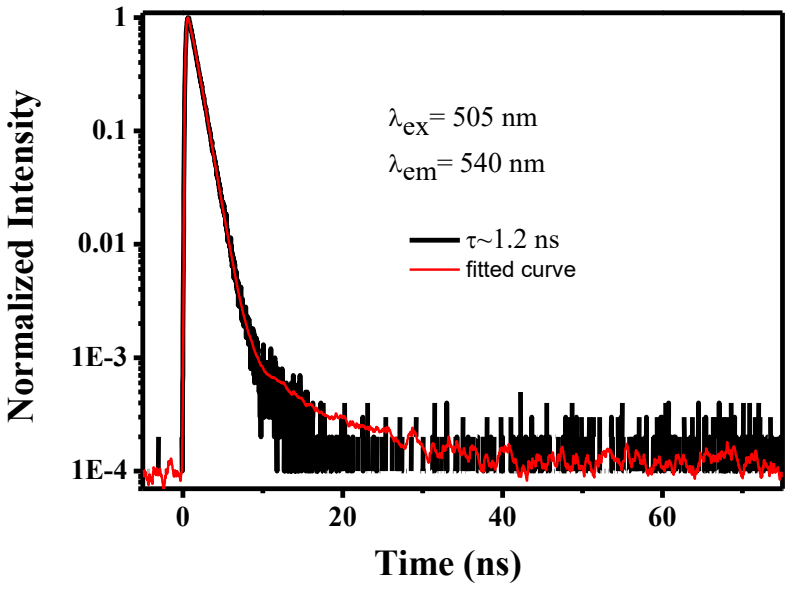

Figure S1: Excited-state decay trace of eosin Y in ethanol saturated with oxygen, λ_{ex} = 505 nm and λ_{em} = 540 nm.

Figure S2.

In this figure, the excitation spectra of eosin Y were taken in HORIBA Fluorolog-3 by using peltier setup in water with varying temperature from 10 ºC to 80 ºC. The emission maxima were taken at 540 nm. It was observed that the intensity increases with increasing temperature.

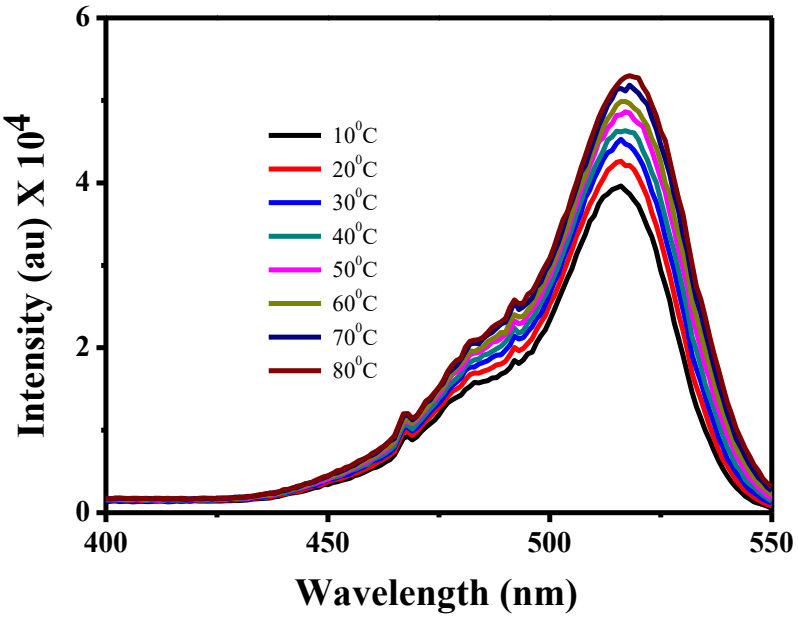

Figure S2: Excitation spectra of eosin Y aqueous solution with varying temperature, λ_{em} = 540 nm.

Figure S3.

Solvent-dependent spectra of eosin Y were recorded, and shifts in the emission were observed across different solvents, which may indicate hybridized local and charge-transfer (HLCT) character. All emission spectra were recorded using excitation at 490 nm, and all experiments were performed on a HORIBA Fluorolog-3 spectrofluorometer.

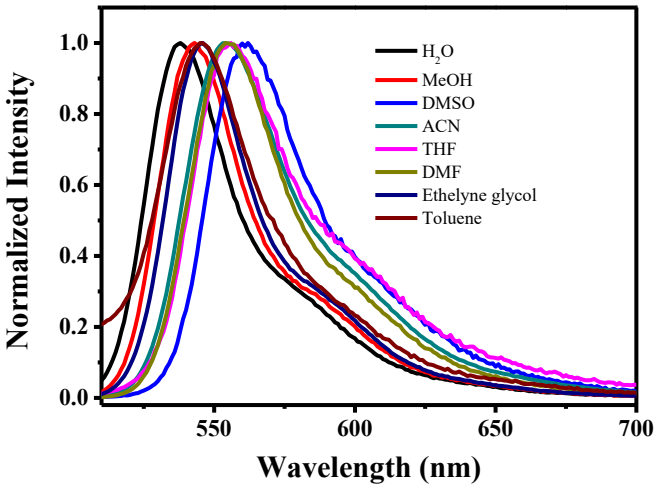

Figure S3. Emission spectra (λ_{ex} = 490 nm) of eosin Y in different solvents.

Figure S4.

Time-resolved emission spectroscopy (TRES) was conducted to obtain the phosphorescence spectrum of eosin Y at 77 K. The spectrum was recorded with a delay time of 100 μs using λ_{ex} = 490 nm. A maximum emission peak around 700 nm was observed, indicating a very low quantum yield. All measurements were carried out using a HORIBA Fluorolog-3 spectrophotometer.

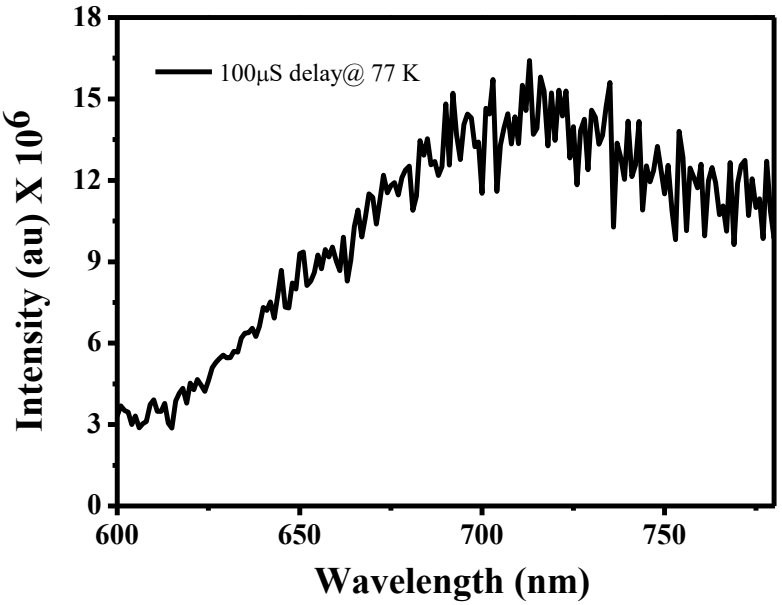

Figure S4. Phosphorescence spectrum (λ_{ex} = 490 nm) of eosin Y in water at 77 K.

Figure S5.

In this figure, the emission spectra of pheophorbide A (PhA) were taken in water, with an excitation wavelength of 490 nm. A temperature independent emission was observed with varying temperature from 10 ºC to 80 ºC.

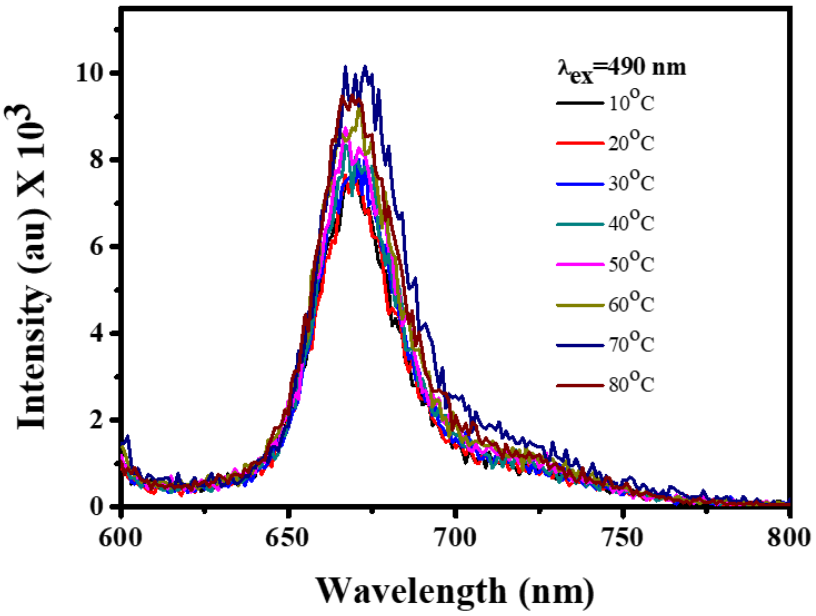

Figure S5. Temperature independent emission spectra of pheophorbide a.

Figure S6.

In this figure, the emission spectra of eosin Y in ethanol were plotted with changing temperature from 5^0C to 60^0C. The emission intensity of eosin Y decreases with increasing temperature when excited at 490 nm.

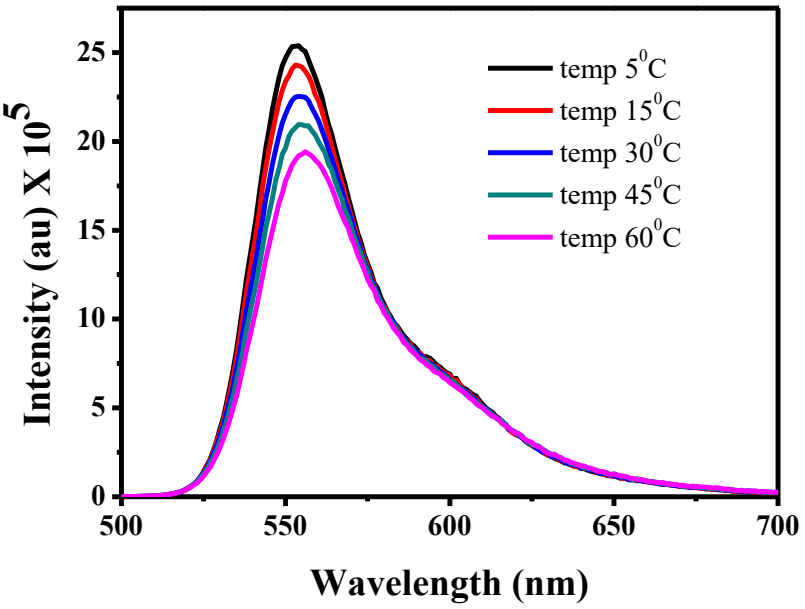

Figure S6: Emission spectra of eosin Y in ethanolic solution with varying temperature, λ_{ex} = 490 nm.

Figure S7.

^{1}H NMR data for eosin y in D_2O and in DMSO-d^6 was given in this following figure. In the D_2O, 5 signals come i.e., 7.25 (1H,d), 7.47 (2H,s), 7.61 (1H,t), 7.66 (1H,t), 7.9 (1H,d) and in DMSO-d6, 7 different proton signals come i.e., 6.91 (2H,s), 7.10 (1H,d), 7.47 (2H,s), 7.78 (1H,t), 7.85 (1H,t), 8.03 (1H,d), 10.84 (1H,s).

(a)

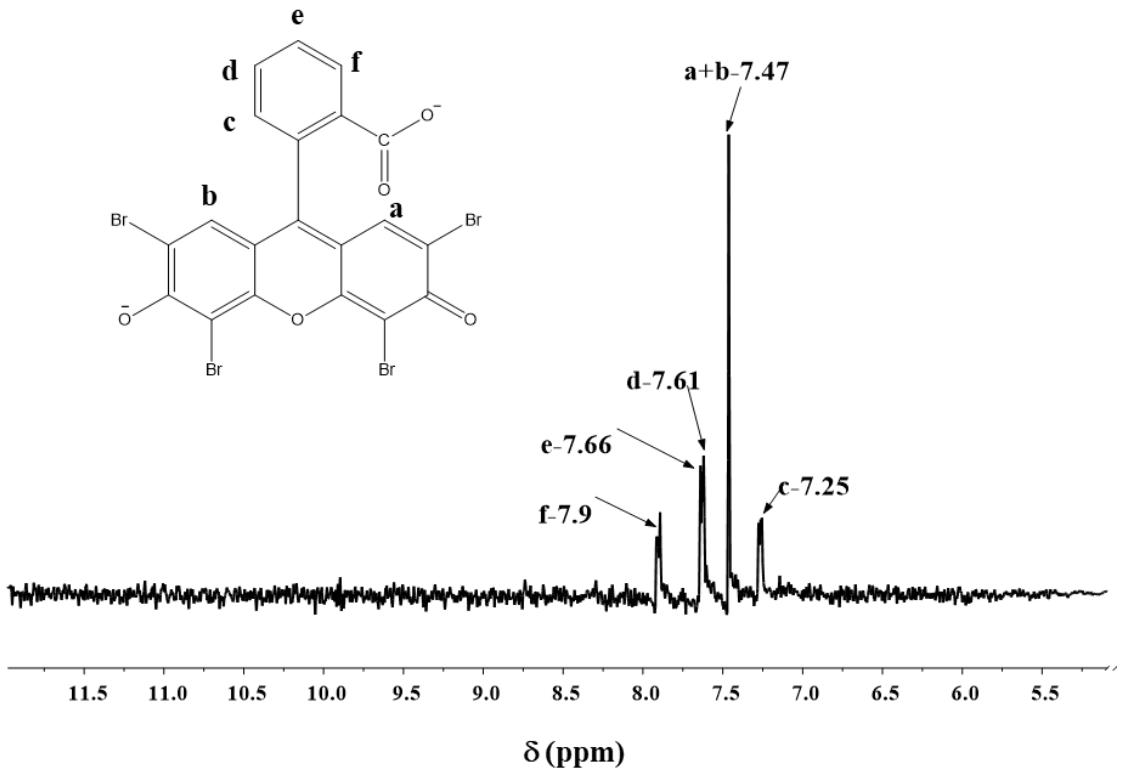

(b)

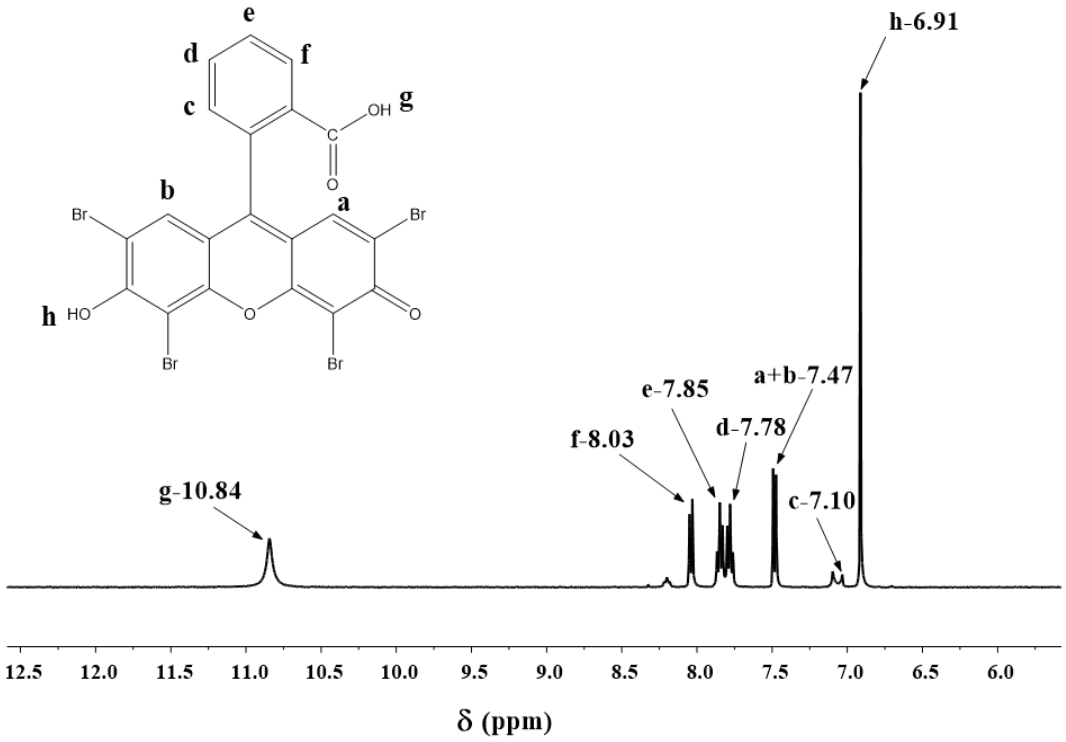

Figure S7: ^{1}H NMR spectra of eosin Y (a) in D_2O (7.25 (1H,d), 7.47 (2H,s), 7.61 (1H,t), 7.66 (1H,t), 7.9 (1H,d)) and (b) in DMSO-d6 (6.91 (2H,s), 7.10 (1H,d), 7.47 (2H,s), 7.78 (1H,t), 7.85 (1H,t), 8.03 (1H,d), 10.84 (1H,s)).

Figure S8.

The optimised structures of eosin y in the two different forms i.e., the neutral quinoid, and dianionic are given in this following figure.

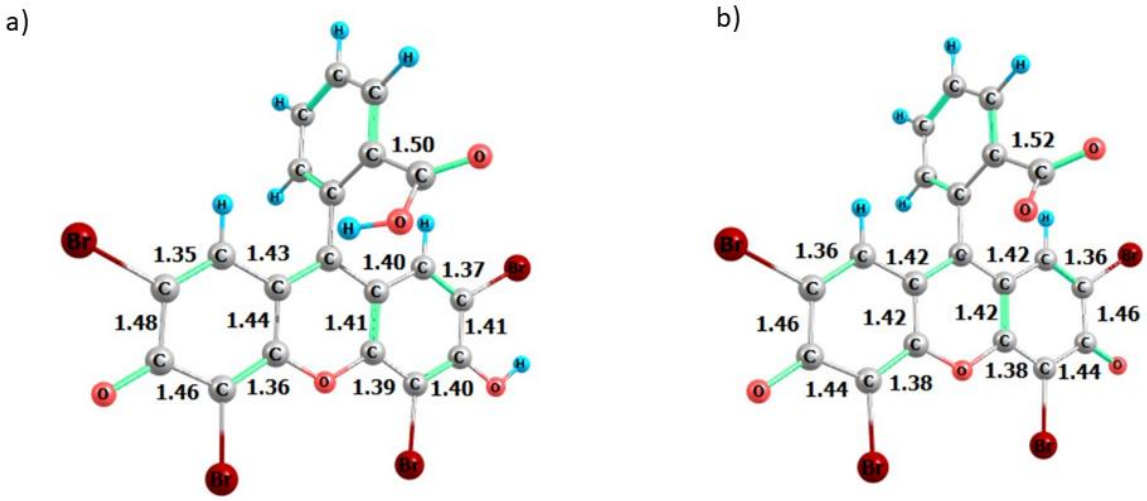

Figure S8. Optimized structures of eosin y in neutral quinoid (a), and dianionic (b) forms. Key bond distances are shown in Å.

Figure S9.

Figure S9 shows the energy levels along with their spin-states for eosin Y in neutral quinoid, and dianionic forms using TD-DFT calculation. It was observed that, the neutral quinoid form has an energy gap between S_1 and T_2 of 0.19 eV, whereas for S_1-S_0 it is 2.48 eV. For dianionic form, the energy gap between S_1 and T_2 was found to be 0.1eV, whereas for S_1-S_0 it was 2.73 eV. The S_0-T_1 gap was found to be 1.74 eV for dianionic form which is in good agreement with the phosphorescence peak max around 705 nm.

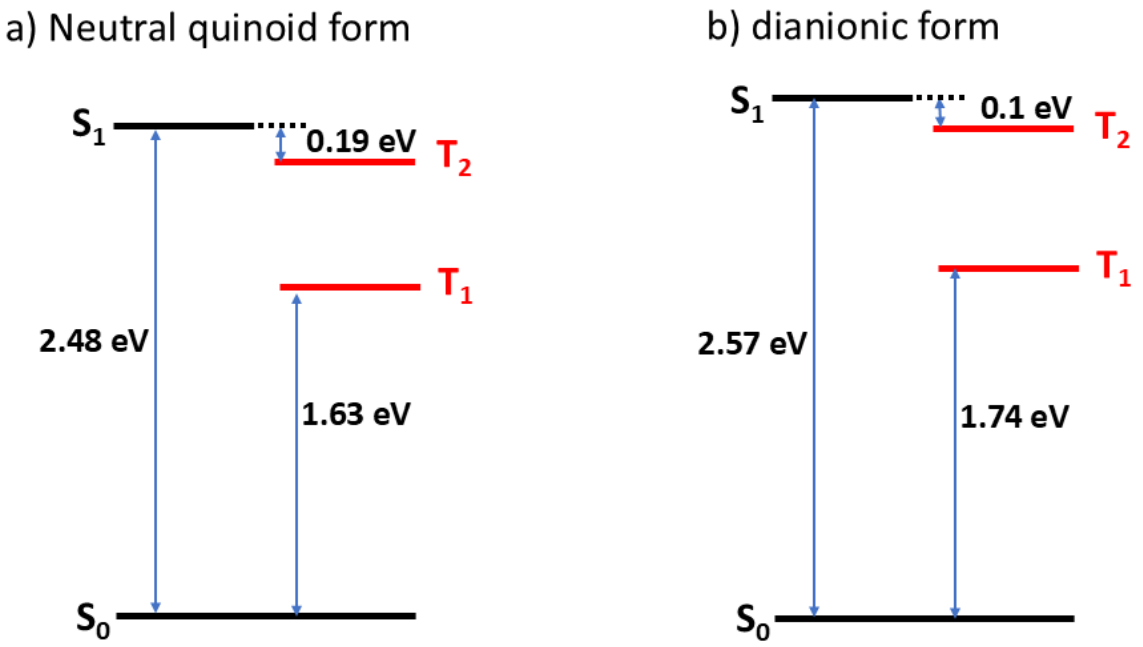

Figure S9. Energy levels along with their spin-states for eosin Y in neutral quinoid, and dianionic forms calculated by TD-DFT at B3LYP/Def2-TZVP level of theory using SMD solvent model. For neutral quinoid and dianionic forms parameters for DMSO and water is used respectively.

Figure S10.

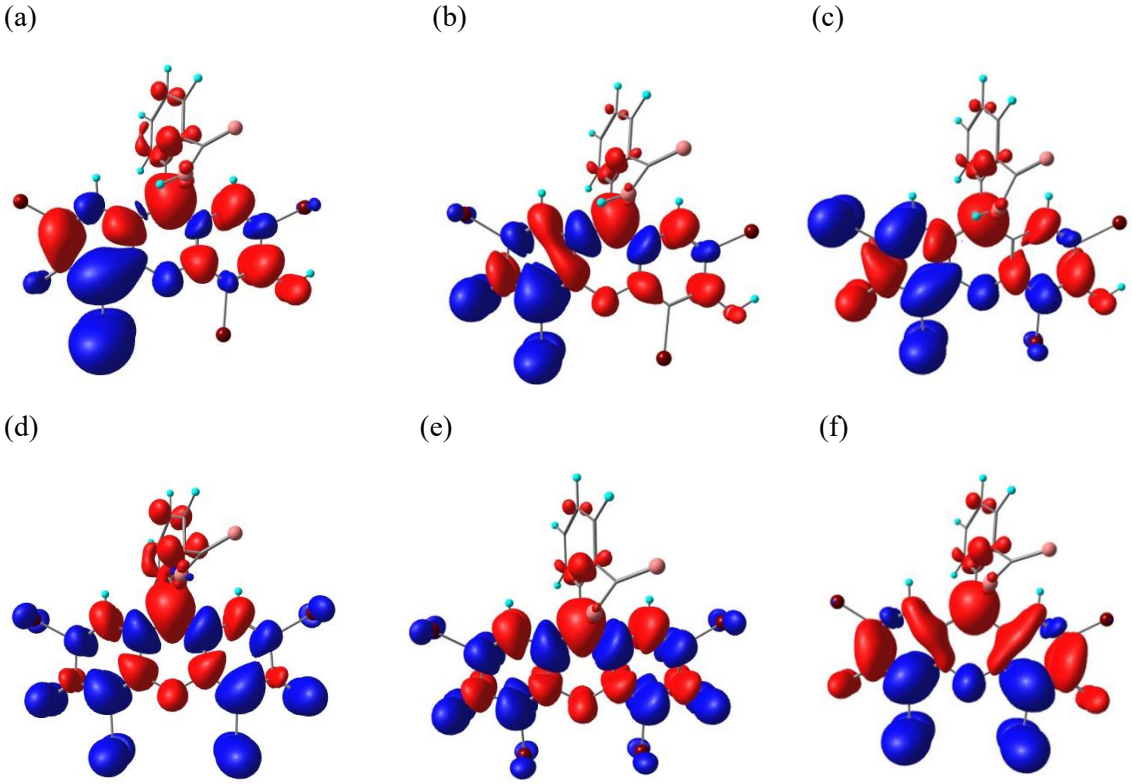

Figure S10. TD-DFT difference density plot (Δρ) for neutral quinoid form in S_1(a), T_1(b), T_2(c) states and same for the dianionic form in S_1(d), T_1(e), and T_2(f) states. The blue (red) regions indicate decrease (increase) in the electron density upon transition. Dianionic form exhibit higher charge separation in the triplet state (T_2) and minimal difference in charge distribution in S_1 and T_1 states.

Figure S11.

Temperature-dependent emission measurements of eosin Y were conducted at varying dye concentrations. Thermal sensitivity was found to increase upon dilution, effectively excluding aggregation as the primary cause of the temperature-dependent behaviour. At higher concentrations, aggregation does occur and suppresses RISC, leading to reduced sensitivity. In all cases, emission intensity increased with temperature. All spectra were recorded using 490 nm excitation on a HORIBA Fluorolog-3 spectrophotometer equipped with a Peltier temperature-control system to ensure precise thermal regulation.

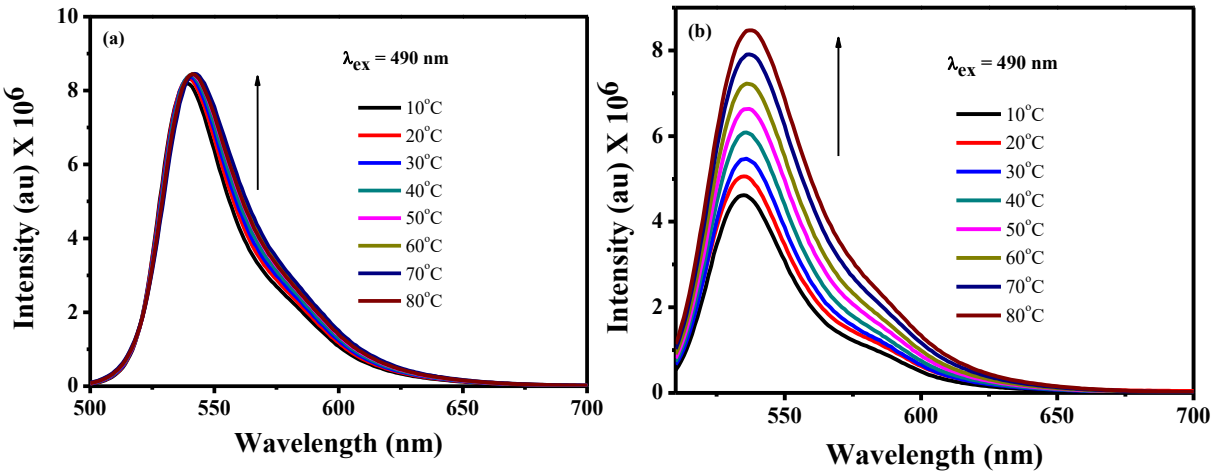

Figure S11. Study of temperature dependent fluorescence intensity of eosin Y solution in water at concentrations a) 1.4 mM and b) 2 µM.

Figure S12.

At a fixed eosin Y concentration in aqueous solution, where emission intensity normally increases with rising temperature, the introduction of 1,3,5,7-cyclooctatetraene (COT), a well-established triplet-state quencher, leads to a clear reversal of this temperature-dependent emission behavior. This observation indicates that the thermal enhancement of fluorescence is mediated by triplet-state processes, specifically involving delayed fluorescence via RISC. All emission spectra were acquired using 490 nm excitation on a HORIBA Fluorolog-3 spectrophotometer equipped with a Peltier temperature-control system to ensure precise thermal regulation.

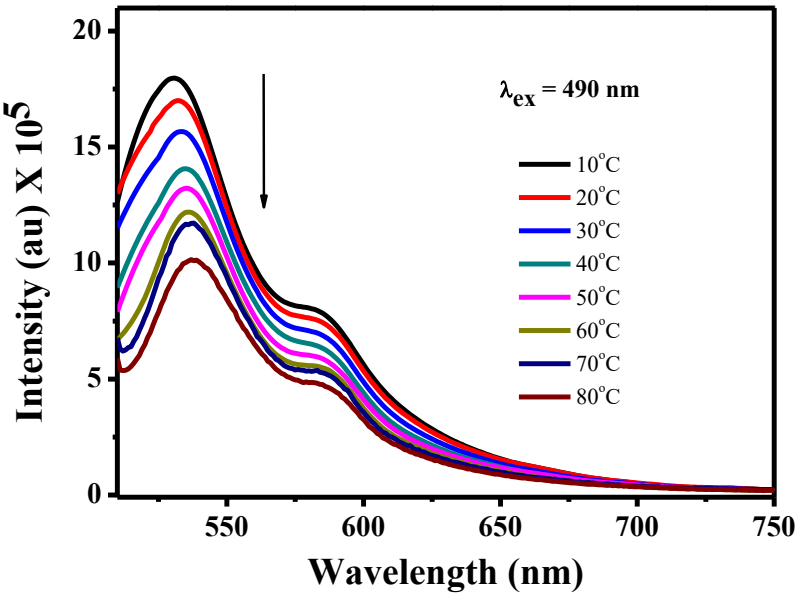

Figure S12. Temperature study of aqueous eosin Y in presence of triplet-state quencher COT.

Figure S13.

The normalized emission and the excitation spectra of eosin y in H_2O and DMSO were presented at 30 ºC and 60 ºC. Neither the emission nor excitation spectra recorded at different temperatures show significant spectral changes. The significant change would be expected if aggregation were responsible for the observed behaviour. This nullifies the presence of aggregation of the dye in different solvents. All emission and excitation spectra were acquired using 490 nm excitation on a HORIBA Fluorolog-3 spectrophotometer.

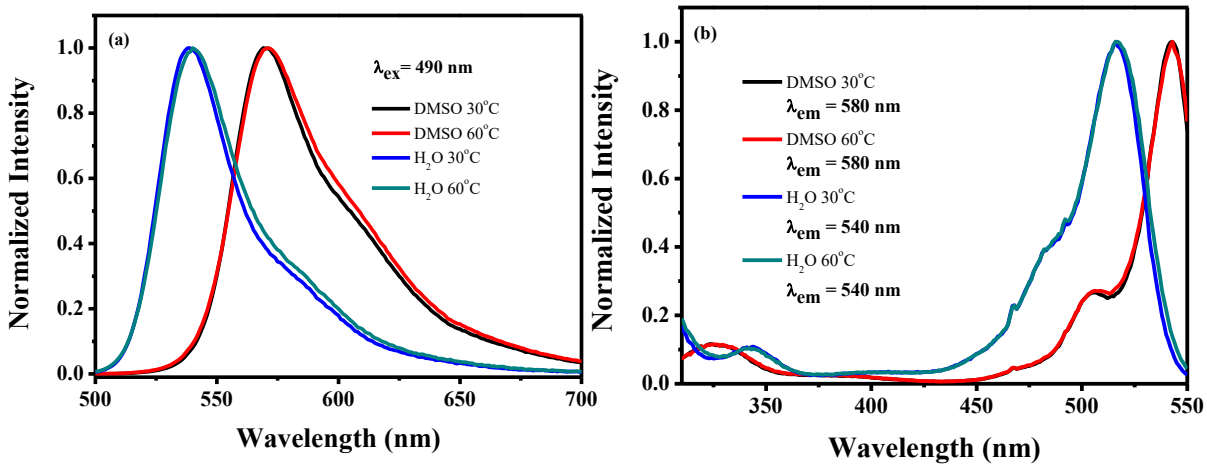

Figure S13. Normalized (a) emission spectra of eosin Y in water and DMSO at different temperature, and (b) excitation spectra of eosin Y in water and DMSO at different temperature.

Figure S14.

FE-SEM image of the AEMH-PS-Ey/PhA nanoparticle was taken in commercially available VP 300 (Carl Zeiss Pvt. Ltd and Merlin) instruments with an opening voltage of 5 KV. Spherical particle was observed with an average particle size of 67.41±8 nm (scale bar – 500 nm).

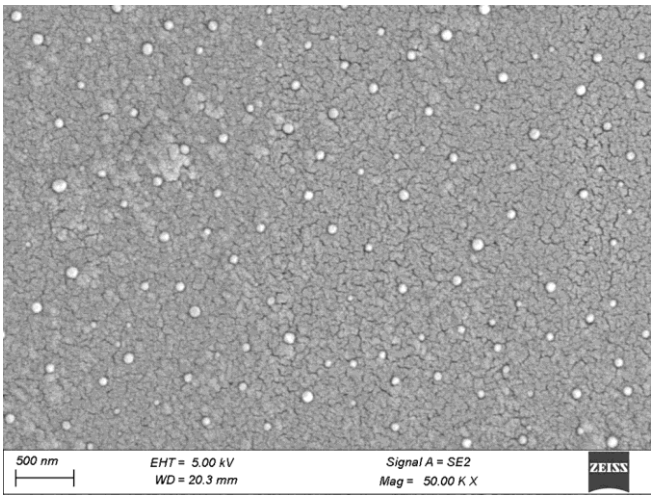

Figure S14. Electron micrograph of AEMH-PS-EY-PhA nanoparticle.

Table S1. Different parameters calculated by TD-DFT at B3LYP/Def2-TZVP level of theory using SMD solvent model.

Form of eosin Y	**Solvent**	**ΔE_{ST}** (eV)	**V_{SOC}** ($S_1 \rightarrow T_2$) (cm^{-1})	**V_{SOC}** ($T \rightarrow S$) (cm^{-1})	**Reorganization Energy** (λ) (eV)
Neutral quinoid	DMSO	0.19	1.09	1.01	0.11
Di-anionic	H_2O	0.10	0.72	0.55	0.07

Table S2.

(a) k_{RISC} and k_{RISC}/k_{ISC} values of eosin Y in neutral quinoid form.

Temperature (K)	k_{RISC} (s^{-1})	k_{ISC} (s^{-1})	k_{RISC}/k_{ISC}[a]	k_{RISC}/k_{ISC}[b]	$\emptyset_{DF}/\emptyset_{PF}$[c]
283	185882.6807	527092516.00	0.000352657	0.02	0.09
293	243290.9731	527092516.00	0.000461572	0.02	0.11
303	312646.1646	527092516.00	0.000593152	0.03	0.14
313	395176.4094	527092516.00	0.000749729	0.04	0.18
323	492056.0006	527092516.00	0.000933529	0.05	0.23
333	604389.6305	527092516.00	0.001146648	0.06	0.28
343	733199.5540	527092516.00	0.001391026	0.07	0.34
353	879415.6213	527092516.00	0.001668427	0.09	0.40

(b) k_{RISC} and k_{RISC}/k_{ISC} values of eosin Y in di-anionic form.

Temperature (K)	k_{RISC} (s^{-1})	k_{ISC} (s^{-1})	k_{RISC}/k_{ISC}[a]	k_{RISC}/k_{ISC}[b]	$\emptyset_{DF}/\emptyset_{PF}$[c]
283	4421322.345	229984648.00	0.019224424	0.44	2.02
293	5021092.006	229984648.00	0.021832292	0.50	2.30
303	5651359.546	229984648.00	0.024572769	0.57	2.59
313	6309533.312	229984648.00	0.027434585	0.63	2.89
323	6993011.109	229984648.00	0.030406426	0.70	3.20
333	7699217.320	229984648.00	0.033477092	0.77	3.52
343	8425632.368	229984648.00	0.03663563	0.84	3.86
353	9169815.516	229984648.00	0.039871424	0.92	4.20

[a] based on calculated ISC values, which were overestimated due to the absence of Franck–Condon factor considerations.

[b] based on experimental ISC value obtained in literature. [46]

[c] based on Equation (2) assuming $\chi_S = 0.2$ [62] and k_{PF} and k_T are 8.3 x 10^8 and 5.2 x 10^3 s^{-1} respectively.

The $\emptyset_{DF}/\emptyset_{PF}$

$$1_M \underset{I_0}{\overset{K_{FM}}{\rightleftarrows}} 1_{M^*} \underset{K_{ISC}}{\overset{K_{RISC}}{\rightleftarrows}} 3_{M^*} \xrightarrow{k_{nr}^T}$$

$\frac{d[3_{M^*}]}{dt} = K_{ISC}\,[1_{M^*}] - K_T\,[3_{M^*}]$ equation (s1)

Applying SSA on $[3_{M^*}]$, $\frac{d[3_{M^*}]}{dt} = 0$

$\frac{[3_{M^*}]_{SS}}{[1_{M^*}]_{SS}} = \frac{K_{TM}}{K_T} \cdot \frac{K_{ISC}}{K_{GT} + K_{RISC}}$ equation (1)

The rate at which prompt photons emit

$R_{PF} = K_{PF}[1_{M^*}]_{SS}$ equation (s2)

The rate at which delayed photons emit considering RISC as the RDS

$R_D = \gamma_S . K_{RISC}[3_{M^*}]_{SS}$ equation (s3)

Thus, $\frac{\varphi_{DF}}{\varphi_{PF}} = \frac{\gamma_S . K_{RISC}[3_{M^*}]_{ss}}{K_{PF}[1_{M^*}]_{ss}}$ equation (s4)

Putting, $\frac{[3_{M^*}]_{ss}}{[1_{M^*}]_{ss}} = \frac{K_{ISC}}{K_T}$ in equation (s4) we get,

$\frac{\varphi_{DF}}{\varphi_{PF}} = \frac{\gamma_S . K_{RISC} K_{ISC}}{K_{PF} K_T}$ equation (2)